Supporting Information

A universal approach to 'host' carbon nanotubes on charge triggered 'guest' interpenetrating polymer network for excellent 'green' electromagnetic interference shielding

*Kunal Manna†, Ria Sen Gupta† and Suryasarathi Bose†,**
†Department of Materials Engineering, Indian Institute of Science, Bengaluru – 560012, India
E-mail: * *Corresponding Author Email address (sbose@iisc.ac.in)*

Supporting Information I (SI-I)

Though, the polymerization mechanism of Dopamine to polydopamine is still not very well established. However, we relied on existing literature for confirming the chemical structure of PDA.[1,2] It was from the reference no.2 mentioned here, that we thought of exploring the idea of stimuli responsive PDA sequential IPN membranes for being the host during construct formation with host-guest assembly architecture.

The polymerization mechanism of Dopamine to polydopamine is still not very well established. However, we completely relied on existing literature for corroborating the polymerization mechanism:

Here,

- DA = Dopamine
- DSQ = Dopamine semiquinone
- DQ = Dopamine quinone
- DAL = Leucodopamine chrome
- DAC = Dopaminechrome
- DHI = 5,6-dihydroxyindole

❖ **DQ to DAL via Michael type intramolecular cycloaddition reaction**

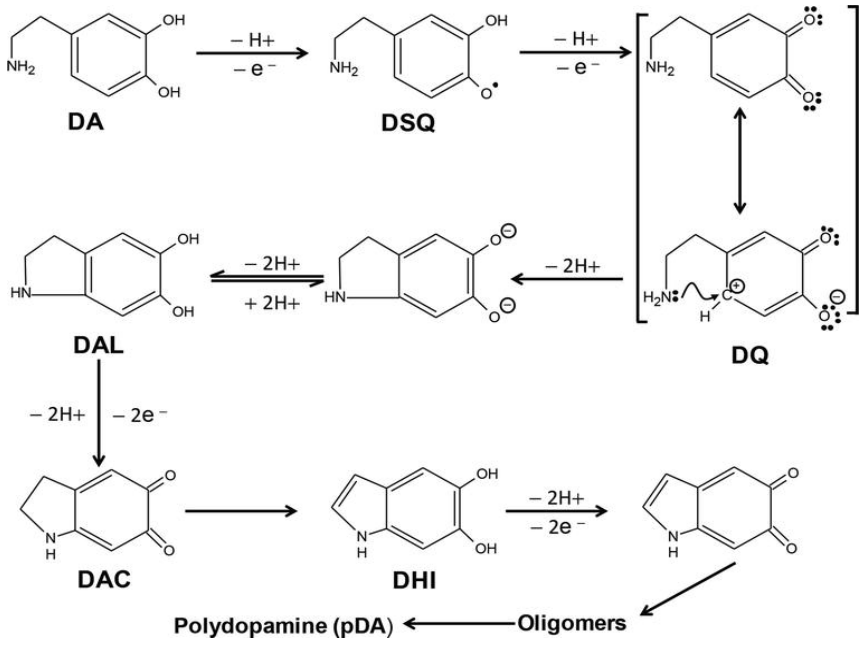

Scheme 1: The polymerization mechanism of Dopamine to polydopamine

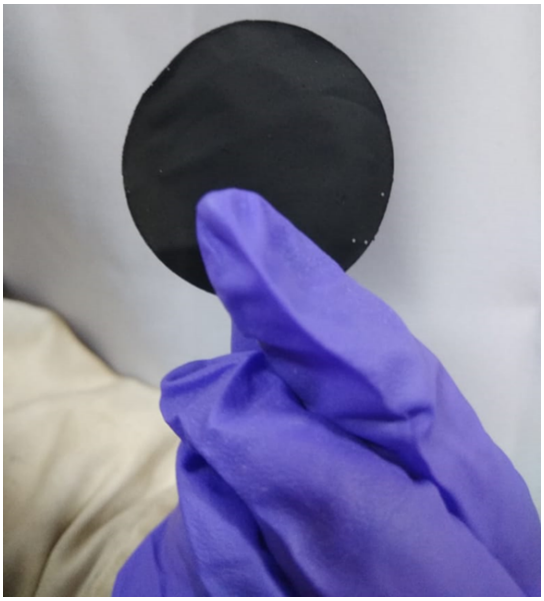

Fig. S1. Digital image of Freestanding ACNT paper obtained from vacuum assisted filtration.

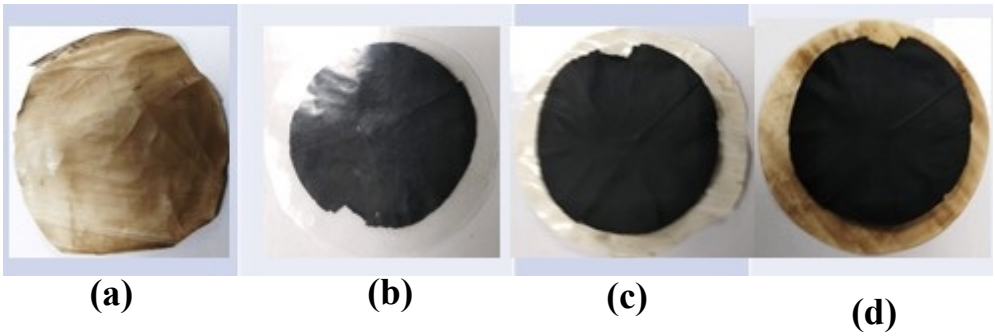

Fig. S2. Digital images of (a) IPN membrane and different control samples (b) control sample-3, C3 (c) control sample-1, C1, and (d) control sample-2, C2.

Supplementary Information II (SI-2)
Characterization of the IPN-CNT construct:

The constructs were characterized via Fourier Transform IR spectroscopy (FTIR) from PerkinElmer Frontier in the range of mid-IR. X-ray photoelectron spectroscopy was performed on Axis Ultra with Al as the monochromatic source (1.486 keV). Morphological studies and elemental analysis were performed using Ultra55 FE-SEM Karl Zeiss scanning electron microscope equipped with an EDX detector and transmission electron microscope (TEM, FEI Technai G2). Thermogravimetric analysis was performed using TA Q500. XRD (X-ray Diffraction) analysis was performed using PANalytical X-Pert PRO instrument equipped with Cu K_α radiation (λ=1.54 A°). The density of the ACNT/PDDA powder was measured using a Helium gas Pycnometer (Model No.- ULTRAPYC 1200e) Quantachrome India. Raman analysis was duly performed using LabRAM HR with CCD detector. The Zeta-potentials of the particles and the membranes were evaluated using a Zeta-potential analyzer (Zetasizer

NanoZS90, Malvern Instruments) and an electro-kinetic analyzer, SurPASS, Anton Par. BET surface area analysis was carried out in MicrotracBEL, Corp and the corresponding data were analyzed using BELSORP Data Analysis Software BELMaster - Ver 7.3.2.0. The electrical conductivities at room temperature of the constructs and control samples were measured on uniformly polished and compression-molded disks of a thickness of 1 mm via an Alpha-N analyzer, Novocontrol (Germany), with Vrms at 1 V in a wide frequency range of 0.1 Hz to 10 MHz. Room-temperature surface conductivities were measured using four-probe method in Keithley 2420-C source meter. Optical profilometry was performed using Polytec MSA-500 Micro-system analyzer. For thermal scan images, a laser beam of 808 nm was used and the scan images were taken using Fluke IR camera (Model – Fluke TI400) at a certain time interval. The EMI shielding properties of the constructs and the control samples were measured using an Agilent vector network analyzer (VNA) in X, K_u and K band (freq. range = 8.2 to 26.5 GHz). The VNA was coupled to a Vidyut Yantra Udyog (model KU7061; S.N. 2454) waveguide. The bending fatigue test was carried out using a home-built bending fatigue test unit with a bending radius and frequency of 10 mm and 1 Hz, respectively.

Supplementary Information III (SI-3)

FTIR Analysis:

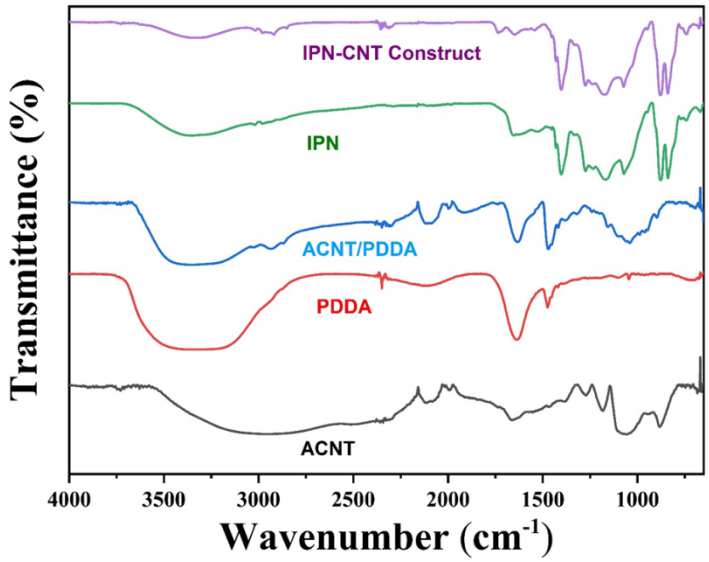

Fig. S3. FTIR Spectra of ACNT, PDDA, ACNT/PDDA, IPN and IPN-CNT

To investigate the structural changes induced via the functionalization of CNT and further conjugating it with IPN membranes for the formation of constructs, FTIR was performed. Figure S2 depicts the composite FTIR spectra for acid functionalized-CNT (ACNT), polyelectrolyte PDDA (used for modifying ACNT), neat IPN membrane, and the IPN-

CNT Constructs. In ACNT, a broad hump of the -OH group is centered around 2613-3054 cm^{-1}. Additionally, a C=O peak at around 1668 cm^{-1} confirms the acid functionalization of the CNTs. PDDA shows representative signals at 3336 cm^{-1} corresponding to $-NR_3^+$ stretching vibration or hydroxyl group. The characteristics bands at 1640 and 1470 cm^{-1} are attributed to the deformation vibration of $-NR_3^+$ and C-H group respectively.[3] The mere presence of peaks at 1630 and 1468 cm^{-1} in ACNT/PDDA further corroborates the successful conjugation of PDDA polymer over the ACNTs. For the IPN membrane, the -OH and -NH groups of catecholamines, produced a distinct and broad peak centered around 3347 cm^{-1}. Due to the bending and scissoring vibrations of the N-H group, two new peaks in the range 1565-1660 cm^{-1} were discovered.[4] The retention of peaks from both IPN and ACNT/PDDA for the IPN-CNT Construct confirms the efficacy of the electrostatic self-assembly.

Supplementary Information IV (SI-4)

BET Plot

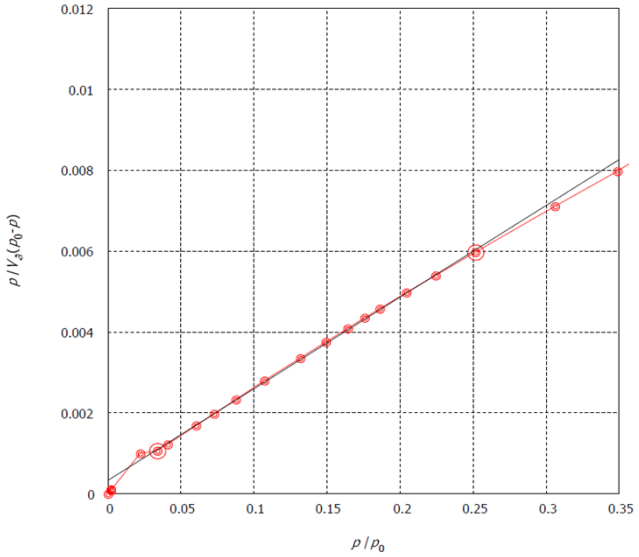

BET-Plot

Adsorptive N2

Adsorption temperature 77.000 [K]

V_m	43.477	[cm³(STP) g⁻¹]	$a_{s,BET}$	1.8923E+02	[m² g⁻¹]
C	67.217		Total pore volume (p/p_0=0.9032)	0.3781	[cm³ g⁻¹]
			Average pore diameter	7.9925	[nm]

Fig. S4. BET Plot and data of ACNT/PDDA.

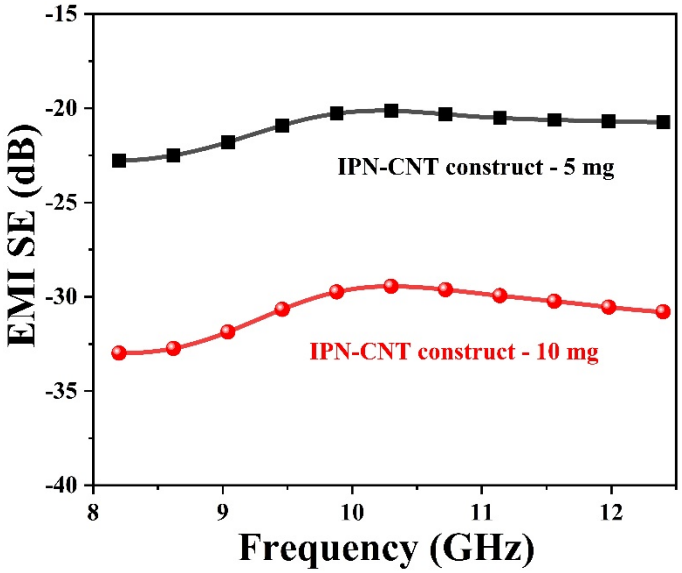

Fig. S5. Plot of EMI SE vs frequency in X-band for IPN-CNT construct corresponding to 5 mg and 10 mg CNT content.

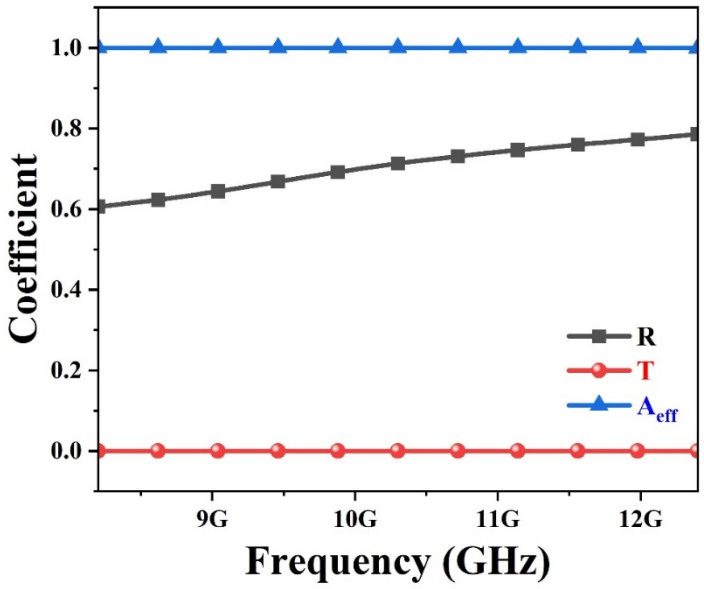

Figure S6: Plot of Reflection (R), Transmission (T) and Effective Absorption coefficient (A_{eff}) vs frequency.

Supplementary Information V (SI-5)

Theory of Electromagnetic Interference (EMI) Shielding

EMI SE is the material's ability to attenuate the energy of the incident electromagnetic waves. When the electromagnetic radiations interact with material under test (shield), the shielding phenomenon is governed by the contributions from reflection (SE_R), absorption (SE_A), and multiple internal reflections (SE_M). The total EMI SE (SE_T) is the sum of the contributions from SE_R, SE_A and SE_M. The total SE_T can be written as;

$$SE_T = SE_R + SE_A + SE_M \quad \text{(S1)}$$

For calculations, SE_M is generally considered negligible when SE_T is higher than 15 dB. In a vector network analyzer, EMI SE is represented in terms of scattering parameters which are S_{11} (forward reflection coefficient), S_{12} (forward transmission coefficient), S_{21} (backward transmission coefficient), and S_{22} (reverse reflection coefficient). The SE_T can be evaluated from the S parameters by using the following equations[5]

$$SE_R = 10log\left(\frac{1}{1-R}\right) = 10log\frac{1}{1-|S_{11}|^2} \quad \text{(S2)}$$

$$SE_A = 10log\left(\frac{1-R}{T}\right) = 10log\frac{1-|S_{11}|^2}{|S_{21}|^2} \quad \text{(S3)}$$

Assuming propagation of EM waves in a nonmagnetic and highly conducting medium, the Fresnel formula for reflection, absorption and multiple reflections, using equation S1, can be given as,

$$SE_T = 10log\left(\frac{1}{T}\right) = 10\log\left(\frac{1}{|S_{21}|^2}\right) = 10log\left(\frac{E_i}{E_t}\right)^2 = 20log\left|\frac{(1+N)^2}{4N}e^{-kd}[1-\left(\frac{1-N}{1+N}\right)^2 e^{2ikt}]\right| \quad \text{(S4)}$$

where E_i and E_t are incident and transmitted intensities of electric field of the EM waves, respectively; N is the complex refractive index of the shield, k is the imaginary part of refractive index, and t is the shield thickness.

From equation S4, the quantitative contributions from SE_R, SE_A, and SE_M are expressed as:

$$SE_R = 20log\left(\frac{(1+N)^2}{4|N|}\right) = 50 + 10log\left(\frac{\sigma}{f}\right) \quad \text{(S5)}$$

$$SE_A = 20log\, e^{-kt} = 20log\, e^{-\alpha t} = 8.686\, \alpha t = 1.7t\sqrt{\sigma f} \quad \text{(S6)}$$

$$SE_M = \left|1-\left(\frac{1-N}{1+N}\right)^2 e^{2ikt}\right| \quad \text{(S7)}$$

In equation S6, α is the attenuation constant indicating the ability of a material to absorb the associated energy of the incident EM waves.

The EMI Shielding efficiency % can be calculated by the following equation.[6]

$$Shielding\ Efficiency\ \% = 100 - \left(10^{\frac{SE}{10}}\right)^{-1} \times 100 \quad \text{(S8)}$$

Where, *SE* stands for total shielding efficiency i.e. SE_T

Further, Skin depth (δ), which explains the intensity of penetration, can be calculated by equation S8 as below:

$$SE_A = -8.686\frac{t}{\delta} \quad \text{(S9)}$$

Where, *t* stands for shield thickness.

The green index (g_s) of shielding material is calculated using Eq. S10 as below:

$$g_s = \frac{1}{S_{11}^2} - \frac{S_{21}^2}{S_{11}^2} - 1 \quad \text{(S10)}$$

Supplementary Information IV (SI-6)

Table S1: Comparison table of SE/t (dB cm^{-1}) of IPN-CNT construct with reported literatures

Sl. No.	Composites	EMI SE (dB)	Thickness	SE/t (dB cm^{-1})	Ref.
1.	MWCNT/Phenolic Composite paper	32.4	140 µm	2314	9
3.	MCMBs/MWCNT/ Fe_3O_4 Paper	80	0.5 mm	1600	11
4.	CNT/Cellulose Paper	20	0.45 mm	888	12
5.	MCMB-MWCNTs Composite Paper	56	0.60 mm	933	14
6.	MWCNT buckypaper	101.7	450 µm	2260	16
8.	**IPN-CNT construct**	**45**	**160 µm**	**2812.5**	**This work**

Table S2: Comparison table of SSE_t (dB cm^2 g^{-1}) of IPN-CNT construct with reported literatures

Sl. No.	Composites	SSE_t (dB cm^2 g^{-1})	Ref.
1.	rGO/MWCNT Sandwich	2259	10
2.	MWCNT/Cellulose Paper	4205	13
3.	Natural rubber/carbon nanotubes composite foams	312.69	15
4.	**IPN-CNT Construct-25**	**1607**	**This work**
5.	**IPN-CNT Construct-10**	**4286**	**This work**
6.	**IPN-CNT Construct-5**	**5715**	**This work**

References

1. Lakshminarayanan, Rajamani, Srinivasan Madhavi, and Christina Poh Choo Sim. "Oxidative polymerization of dopamine: A high-definition multifunctional coatings for electrospun nanofibers-an overview." Dopamine-Health and Disease (2018): 113-132.
2. Pérez-Mitta, Gonzalo, Jimena S. Tuninetti, Wolfgang Knoll, Christina Trautmann, María Eugenia Toimil-Molares, and Omar Azzaroni. "Polydopamine meets solid-state nanopores: a bioinspired integrative surface chemistry approach to tailor the functional properties of nanofluidic diodes." Journal of the American Chemical Society 137, no. 18 (2015): 6011-6017.
3. Celestino, G. G. *et al.*, Adsorption of gallic acid on nanoclay modified with poly(diallyldimethylammonium chloride). *Environ. Sci. Pollut. Res.* **26,** 28444–28454 (2019).
4. Muchtar, S., Wahab, M., Mulyati, S., Riza, M. & Arahman, N. Deposition of polydopamine on the surface of Polyvinylidene Fluoride (PVDF) membrane as A UV-Shielding layer. *IOP Conf. Ser. Mater. Sci. Eng.* **523,** (2019).

5. Iqbal, A. *et al.* Anomalous absorption of electromagnetic waves by 2D transition metal carbonitride Ti_3CNT_x(MXene). *Science (80-.).* **369**, 446–450 (2020).
6. Lee, J. *et al.* Ultrahigh electromagnetic interference shielding performance of lightweight, flexible, and highly conductive copper-clad carbon fiber nonwoven fabrics. *J. Mater. Chem. C* **5**, 7853–7861 (2017).